EXCLI Journal 2005;4:61-76 – ISSN 1611-2156
received: 31. August 2005, accepted: 7. September 2005, published: 16. September 2005

Original article:

Biological and structural characterizations of mutations in X-linked spondyloepiphyseal dysplasia tarda

Mi Suk Jeong, Kyoung Mi Lee, and Se Bok Jang*

Korea Nanobiotechnology Center, Pusan National University, Jangjeon-dong, Keumjeong-gu, Busan 609-735, Phone: +82-51-510-2523, Fax: +82-51-581-2546, E-mail: sbjang@pusan.ac.kr (*corresponding author), Korea.

ABSTRACT

Spondyloepiphyseal dysplasia tarda (SEDT), an X-linked genetic disease manifesting itself in a disproportionate skeletal structure, is caused by mutations in the SEDL gene. Four missense mutations (S73L, V130D, F83S, and D47Y) have been identified by molecular diagnosis as disease-causing SEDT. Nevertheless, how SEDL mutations disrupt the skeletal structure and cause disease remains unknown. We report here the cloning, expression, and characterization of three different missense mutations (S73L, V130D, and D47Y) in mouse SEDL. The overexpression of the D47Y mutation was mainly observed in the supernatant but those of the S73L and V130D mutations are shown in the insoluble pellets. The substitution of the S73L mutation induces the exposure to hydrophobic amino acids and causes aggregation. That of V130D might break hydrophobic interaction and decrease the secondary structure. The CD spectra of three mutants (S73L, V130D, and D47Y) showed that the α-helices decreased more than that of wild-type SEDL. The F83S (stop) mutant might suggest a large conformational change as the mutant V130D. In order to visualize conformational changes in mutated structures, we used molecular modeling techniques minimizing the total energy. These results could provide the biological characterization and conformational information of the SEDL mutants and suggest the clinical severity of the disorder among human SEDL patients.

Keywords: SEDL, missense mutations, expression, CD analysis, modeling

INTRODUCTION

The X-linked form of SEDT, a radiologically distinct skeletal dysplasia affecting the vertebrae and epiphyses, is caused by mutations in the SEDL gene. This progressive skeletal disorder, which manifests itself in childhood, is characterized by disproportionately short stature with short neck and trunk, barrel chest, and the absence of systemic complications (Bannerman et al. 1971, Iceton et al. 1986, MacKenzie et al. 1996). SEDL is widely expressed in tissues including fibroblasts, lymphoblasts and fetal cartilage (MacKenzie et al. 1996). The SEDL gene in Xp22 is composed of six exons and spans a genomic region of approximately 20 kb. It encodes a protein of 140 amino acids and plays a role in vesicular transport from the ER to the Golgi complex (Gedeon et al. 1999, Sacher et al. 2001). The recent finding that a defect in the protein sedlin, whose yeast counterpart is involved in the first step of the secretory pathway, leads to a cartilage-specific disorder in humans, raises numerous questions and interesting possibilities for understanding both the pathobiology involved and the role of membrane trafficking in normal cartilage development (Sacher 2003).

Different mutations in patients have been identified along the entire length of the SEDL ORF (420-bp open reading frame); these include nonsense mutations, missense mutations, deletions, insertions, and splicing errors (Shi et al. 2002, Fiedler et al. 2002, Shaw et al. 2003, Xiao et al. 2003, Shaw et al. 2004, Fiedler et al. 2004, Bar-Ysef et al. 2004). The pathogenetic consequences of SEDL mutations are still mostly unknown on the molecular level. Recently, the crystal structure of a 2.4 Å resolution mouse SEDL was isolated by X-ray analysis (Jang et al. 2002). In that structure, three residues (S73, V130, and F83) were buried with low solvent accessibility and located at structurally important sites where the mutations would disrupt the structure. The D47 residue was exposed on the surface of the protein, which area is the major area of interactions with a partner protein (Fig. 1). SEDL mutations can perturb an intracellular pathway that is important in cartilage homeostasis. However, how those replacements of each of the four amino acids in wild-type SEDL disrupt functional interaction is still unknown.

We report here the sub-cloning, expression, purification, CD analysis, and modeling of SEDL mutations. This information could allow the biological characterization of the SEDL mutations and suggest the clinical severity of the disorder among human SEDL patients.

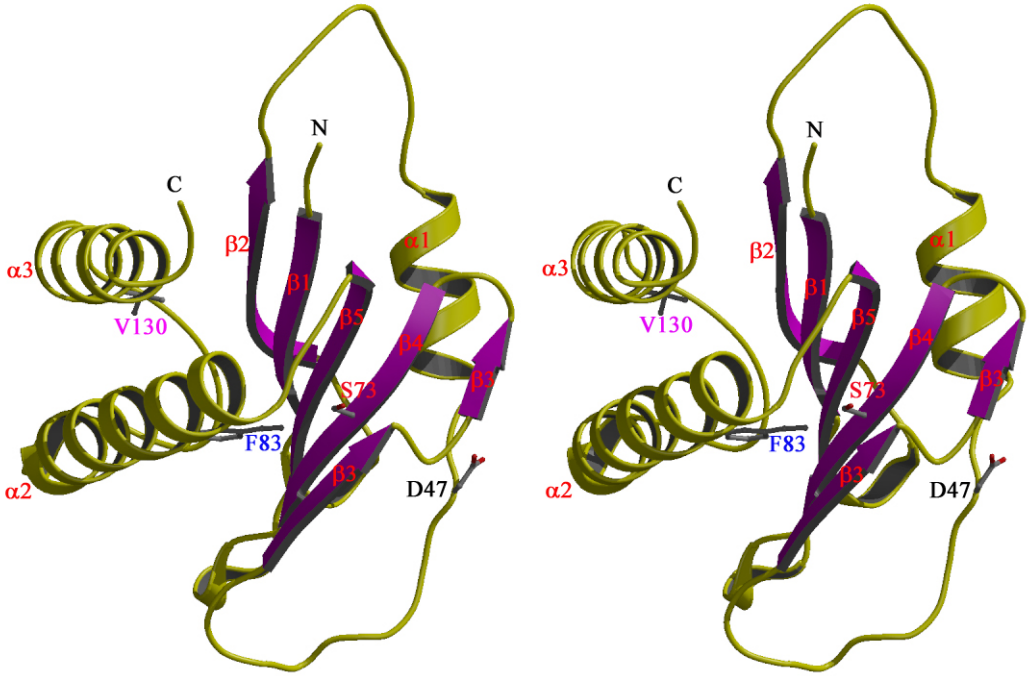

Figure 1: The stereoview of the ribbon diagram of the SEDL monomer
The four side chains of missense mutations are represented by ball and stick, respectively. The SEDL monomer adopts a mixed three α–helices / five β-sheets topology with the β–sheets (shown in magenta) surrounded by the α–helices (shown in yellow).

Materials and Methods

Site-specific mutagenesis

The full-length encoded mSEDL gene (140 amino-acids) was amplified from a mouse cDNA library using the polymerase chain reaction (PCR) technique. The PCR products were purified, digested with *XhoI* and *BlpI*, and then ligated into the pET15b vector (Novagen). The three SEDL mutations selected for the present study consisted of three missense mutations, C218T (S73L), T389A (V130D), and G139T (D47Y). Site-specific mutagenesis was performed using a Quickchange site-directed mutagenesis kit (Stratagene). The stop codon in the F83S mutation was created at the primer for the sub-cloning. The S73L, V130D, and D47Y mutants were amplified with forward and reverse oligonucleotide primers from the recombinant pET15b vector/SEDL plasmid, respectively, using the PCR technique. For S73L, the forward primer was 5'-CGCTCGAGATGTCTGGGAGC TTCTACTTTGTAAT- 3', and the reverse primer was 5'-GGAATTCGCTGAGCCT

AGCTTAAAAGGTGTTTCTTCCC-3'. For V130D, the forward primer was 5'-TCGACAGGAAAGACCAGTTTCTTGG-3', and the reverse primer was 5'-CCAAGAAACTGGTCTTTCCTGTCGA-3'.For D47Y, the forward primer was 5'-ATGCTGCTCTTTTACCTTGTGGACG A-3', and the reverse primer was 5'–TCGTCCACAAGGTAAAGAGCAGCAT –3'. The PCR amplifications were performed using a procedure of 16 cycles of reaction with denaturing at 95 ^{o}C for 30 sec, annealing at 55 ^{o}C for 1 min, and extension at 68 ^{o}C for 6 min. The 4,400 bp band was generated from PCR product using 1% agarose gel electrophoresis. After the PCR, the amplified DNA fragments were ligated by T4 DNA ligase. The ligation mixture was used to transform competent cells of *E. coli* XL1-blue. The colonies were isolated, and the plasmids were obtained using Qiagen miniprep kits. All of the DNA sequences of the mutated genes were verified by sequencing.

Expression and purification

Mouse SEDL was expressed in the *Escherichia coli* strain BL21(DE3)RIL and purified as previously described (Jang et al. 2002b). The cells were initially grown in 50 mL of LB-ampicillin (50 μg/ml) and chloramphenicol (170 μg/ml) overnight at 37 ^{o}C. Inoculars were added to 2 L of LB-ampicillin and chloramphenicol. The large cultures were immediately moved to an incubator and stored at 37 ^{o}C. When the culture reached an A_{600} of 0.5-0.7, isopropyl β-D-thiogalactopyranoside (IPTG) was added at a final concentration of 1 mM to induce 6x His-tagged SEDL mutants as well as wild-type SEDL. After 4-6 h, the cells were harvested and D47Y was lysed by sonication in an equilibrium buffer (50 mM Tris-HCl [pH 7.5] and 200 mM NaCl). The supernatant of the D47Y SEDL was used for purification, but for the S73L and V130D mutations, insoluble pellets were used. Inclusion bodies of the S73L and V130D were obtained by sonication and resuspended in a buffer (25 mM Tris-HCl [pH 8.0], 100 mM NaCl, and 1 mM DTT) containing 6 M urea. Each inclusion body solution was added to a refolding solution (100 mM NaCl, 25 mM Tris-HCl [pH 8.0], and 1 mM DTT). The wild-type SEDL and its three mutations were purified as an $(His)_6$-tagged fusion protein at the N terminus and obtained after cleavage by thrombin (Figure 2b). All of the purifications required the nickel-nitriltriacetic acid (Ni-NTA) column (Qiagen), the Resource Q anion exchange column (Amersham Biosciences), and the Superdex 75 column (Amersham Biosciences). The purity of the purified SEDL was determined by sodium dodecyl sulfate-polyacrylamide gel electrophoresis (SDS-PAGE) with 4% (w/v) stacking and 12% (w/v) resolving gels, as described by Laemmli. The

protein solutions were concentrated to 5- 10 mg/ml using a Vivaspin 20 (Satorius).

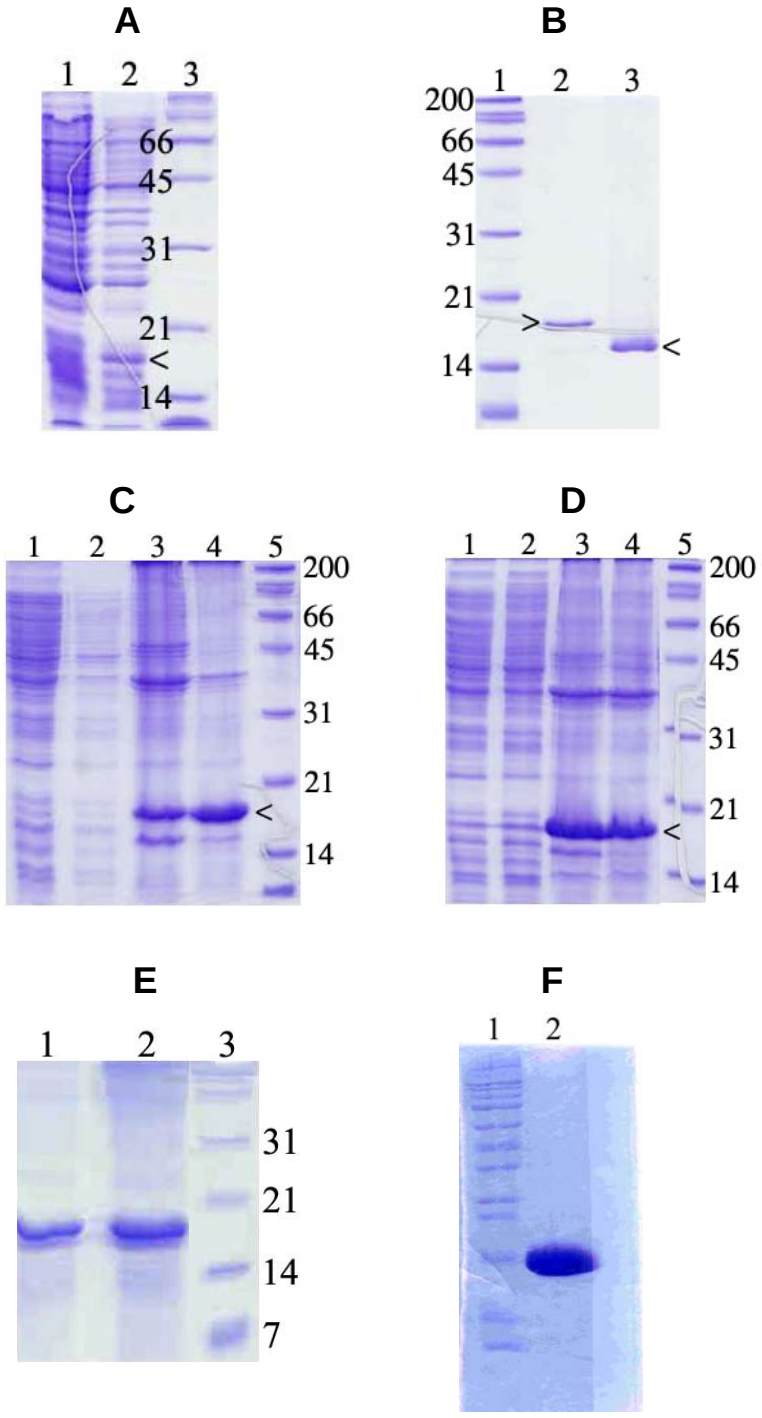

Figure 2: SDS-PAGE analysis of the SEDL mutant expressed in *E. coli*
a) Lanes 1 and 2, supernatants of lysed bacteria of D47Y SEDL before and after induction by IPTG, respectively; Lane 3, molecular weight markers b) Cleavage test of the His-tagged D47Y SEDL. Lane 1, markers; Lanes 2 and 3, D47Y SEDL (18 KDa) before and after His-tag cleavage (16 KDa, 6 mg/ml),

respectively c) Lanes 1 and 2, S73L supernatants before and after induction, respectively; Lanes 3 and 4, S73L pellets before and after induction, respectively; Lane 5, markers d) Lanes 1 and 2, V130D supernatants before and after induction, respectively; Lanes 3 and 4, V130D pellets before and after induction, respectively; Lane 5, markers e) Lanes 1 and 2, refolded S73L (3 mg/ml) and V130D (4mg/ ml) mutants, respectively; Lane 3, markers f) concentrated wild-type SEDL protein (14 mg/ml)

MALDI-TOF analysis

For in-gel digestion, 10 ul of trypsin solution (2 ng/L in 25 mM of ammonium bicarbonate [pH 8.0]) was added and digested at 37 ^{o}C overnight. Peptides were extracted with 50% ACN/0.2% TFA (trifluoroacetic acid) and dried under vacuum for 2 h, followed by reconstruction with 3 ul of CHCA (α-cyano-4-hydroxycinnamic acid) matrix solution (8 mg of CHCA in 1 ml of 50% ACN/0.2% TFA; Gharahdaghi et al. 1999). One microliter of reconstructed sample was loaded on a 96×2 MALDI plate. The peptide mass was acquired with the Voyager DE-PRO (Applied Biosystems, Framingham, MA) in a reflector mode under 20,000 V of accelerating voltage, 76% grid voltage, and 0.002% guide-wire voltage. Cal Mix 2, of the MALDI-MS calibration kit (Applied Biosystems, Framingham, MA), was used for the external calibration, and autolysis fragments of trypsin were used for the internal calibration. Peptide matching and protein searches were performed with the Mascot peptide mass fingerprint (Fig. 3).

Far-UV CD spectroscopy analysis

Circular Dichroism (CD) spectroscopy was used to identify how much the secondary structure was affected by the replacement of three amino acids in wild-type SEDL. The CD spectra of the purified wild-type and mutant proteins were measured from 200 to 260 nm using a 0.05 cm pathlength cell at ambient temperature and a JASCO J-715 spectropolarimeter. Each spectrum was the average of five scans. Far-UV CD spectra were taken at the protein concentration of 0.5 mg/ml. The CD spectra were obtained in milli-degrees and converted to molar ellipticity prior to the secondary structure analysis. The far-UV CD spectra of the mutant and native proteins are shown in Figure 4.

Molecular modeling

The models of the four different missense mutations (S73L, V130D, F83S, and D47Y) in mouse SEDL were constructed using O program (Jones et al. 1991). Refinement to minimize the total energy of the models was performed with the CNS package (Brunger et al. 1998). The

root mean square deviation (rmsd) differences from ideal geometries for bond lengths and angles were calculated with CNS. The overall stereochemical quality of the final models for the mutations of SEDL were assessed by the program PROCHECK (Laskowski et al. 1993).

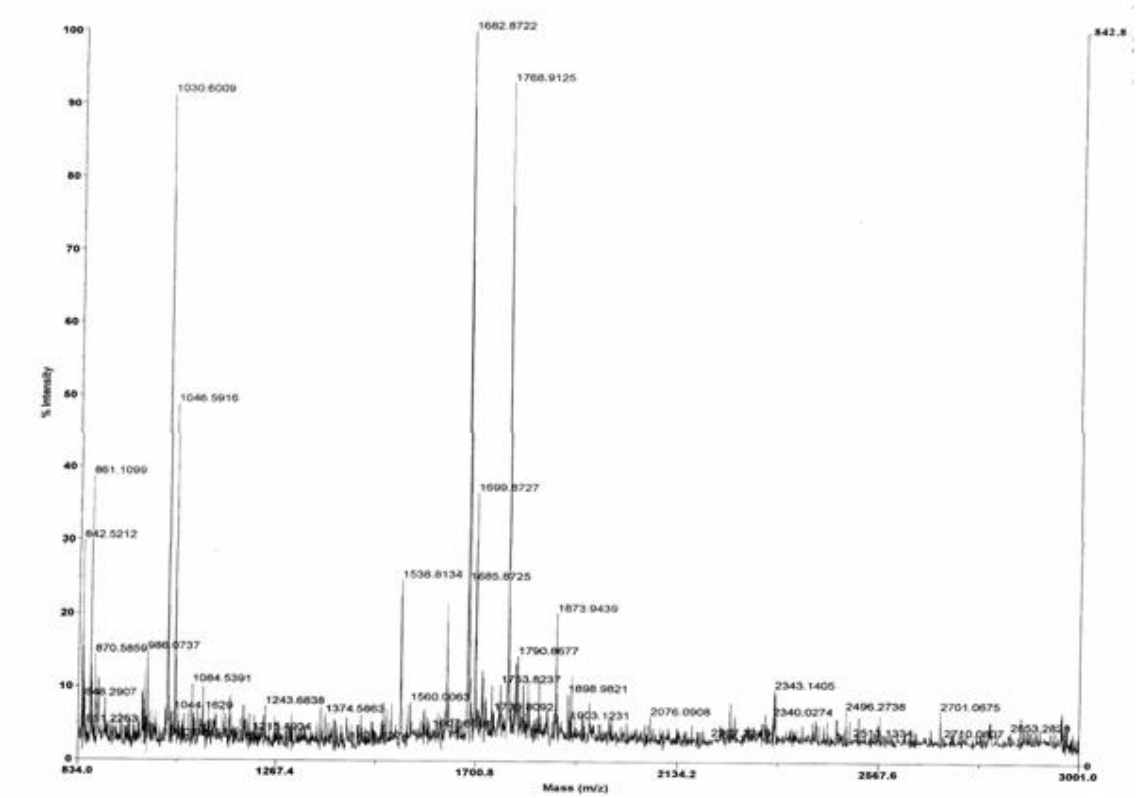

Figure 3: MALDI-TOF mass spectrum analysis
MALDI-TOF peptide spectrum of mouse D47Y SEDL

RESULTS AND DISCUSSION

SEDL appears to be an evolutionarily conserved protein, as its homologues have been identified in mice and humans (Gedeon et al. 1999). SEDT is caused by production of a probable nonfunctional form of SEDL caused by mutations in the SEDL gene located at human chromosome Xp22. Four different missense mutations in SEDL, S73L, V130D, F83S, and D47Y, are responsible for SEDT. Those four mutations are completely conserved in mice and humans. Recently, the SEDL protein crystal structure has been determined and confirmed sites of four different mutations (Fig. 1; Jang et al. 2002a). Nevertheless, the function of SEDL and its role in bone metabolism remains unknown. Also, how SEDL mutations cause the rare osteochondrodysplasia is not known.

Several methods to predict the structure and function of proteins have suggested a significant change (Grunebaum et al. 2001).

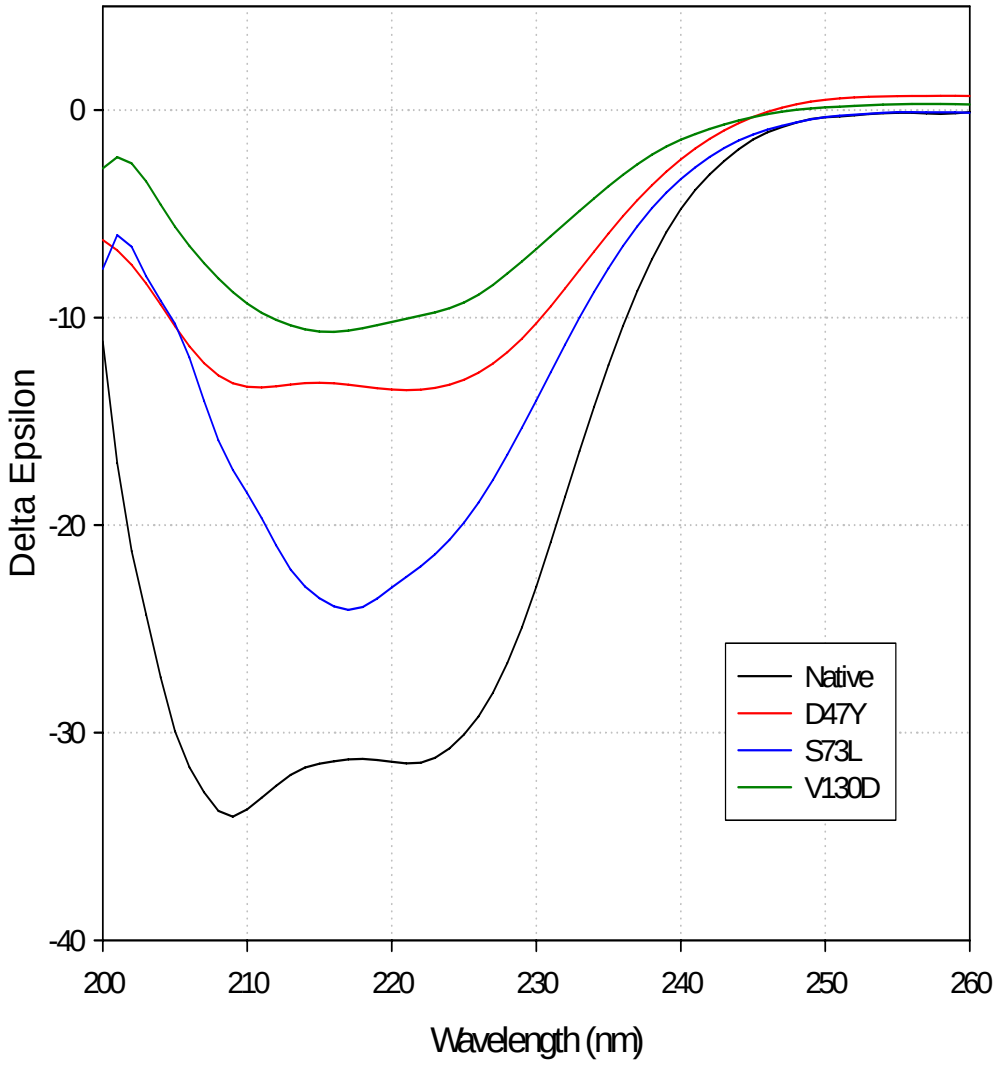

Figure 4: Circular dichroism spectra of SEDL and its variants
The CD spectra were measured from 260 to 200 nm using a 0.05 pathlength cell and the CD signals were merged to CDNN. The color scheme includes wild-type SEDL represented in black, S73L in blue, V130D in green, and D47Y in red.

To study the physiological functions of mutant SEDL, the wild-type and mutated SEDL genes of mice were constructed and expressed in *E coli*. The pET-15b vector was used in the expression of His-tagged fusion SEDL constructs at the N terminus. The constructs were transformed into the expression host *E. coli* BL21(DE3)RIL, and the protein expressions were induced by 1 mM of IPTG. An SDS-PAGE

analysis of the SEDL mutations is shown in Figure 2. We found that there were different effects of the mutations on protein expression and protein solubility. The expression of the D47Y protein was clearly shown in the supernatant but those of the S73L and V130D proteins were mainly observed in the insoluble pellets (Figs. 2a, c and d). The expressions of the S73L and V130D mutations showed a marked decrease by aggregation in an SDS-PAGE analysis. Inclusion bodies of the S73L and V130D mutations were refolded and purified.

MALDI-TOF study of D47Y mutant revealed the approximate molecular mass of the recombinant protein, which was in accordance with the theoretical mass prediction for the SEDL protein with the peptide mass tolerance (50 ppm). Mass-fingerprinting analysis of the proteins were carried out by subjecting them to trypsin digestion. The monoisotopic masses obtained for the individual peptides were in the range of 800-3,000 Da. The sequences of the digested peptides were matched (masses matched No. 6/44, molecular weight 16440.9 Da, accession No. Q9CQP2, and pI 6.02) with the protein sequences in the database using the PROFOUND program. The spectra of the peptide masses obtained for SEDL are shown in Figure 3. The result showed that molecular weight of the mutated D47Y SEDL was almost identical to that of the wild-type protein, by ultracentrifugation analysis, of 16205.3 Da. An ultracentrifugation analysis further evidenced the monomerization of SEDL in solution (data not shown).

To investigate the effect of mutations on the structural integrity of the SEDL protein, CD spectra were obtained for each mutant as well as for wild-type SEDL. The CD spectra of the SEDL mutants showed that each mutation affected the conformation of SEDL to a different extent (Fig. 4). The three mutations (S73L, V130D, and D47Y) induced significant structural changes compared with the wild-type. The CD spectrum of the wild-type SEDL exhibited a negative maximum at about 208 nm and a broad shoulder peak at about 222 nm, which is a typical pattern of α-helix protein. The CD spectrum of the purified S73L exhibited only a negative peak at 217 nm. The mutant S73L maintained the α–helices except α4 disruption and interacted with water molecules (S13). The β–strands pattern of the S73L was different from the case of V130D and D47Y by CD spectra. The V130D mutation had significantly unfolded in the α-helices regions (α2 and α3), and the β–strands and random coils were increased (Table 1). The CD spectral shape of D47Y, except for the negative peak depth, resembled the wild-type spectrum. The D47Y mutation had conformational

change in the longest loop region including the α1-helix and β3-strand connected at both loop termini. D47Y substitution induces the exposure of the bulky polar amino acids, removes a charge from a surface-exposed residue, and can interfere with the protein-protein interaction required for normal function.

Table 1: The contents of the secondary structures of the wild-type and SEDL mutants by CD spectra

Proteins	wild-type SEDL	S73L	V130D	D47Y
α-helices (%)	91.4	78.6	73.6	73.0
β-sheets (%)	0.1	3.4	4.5	5.0
β-turn (%)	8.4	15.8	15.7	17.3
random coil (%)	0.1	2.2	6.2	4.7

The three mutants studied by CD showed that the secondary structure was more or less lost by mutation. This loss of the secondary structures in the proteins can be observed either by local structural perturbation or by increasing the unfolded fraction of a protein. However, it is not clear whether the structural change is localized around the mutation site or not. Several programs used to predict secondary protein structure, GOR IV (Garnier et al. 1999), HNNC (Guermeur), and Predator (Frishman et al. 1996), indicated that the F83S mutation would significantly alter the SEDL structure and introduce an additional alpha helix (Grunebaum et al. 2001). They suggested that a phenotype/genotype correlation is difficult to determine; however, an amino acid change that does not alter the rest of protein may not be as detrimental to the phenotype as a mutation that results in truncation of the protein. The affected patients in the family described there had very mild clinical symptoms. Contrary to other pedigrees with X linked SEDL, in which females heterozygous for the gene defect suffered from subtle skeletal abnormalities and arthritis by middle age (Whyte et al. 1999, Bannerman et al. 1971), the female carriers in the family described here had no objective evidence of SEDL. This may reflect the subtle impact of the C→T mutation on SEDL protein function (Grunebaum et al. 2001).

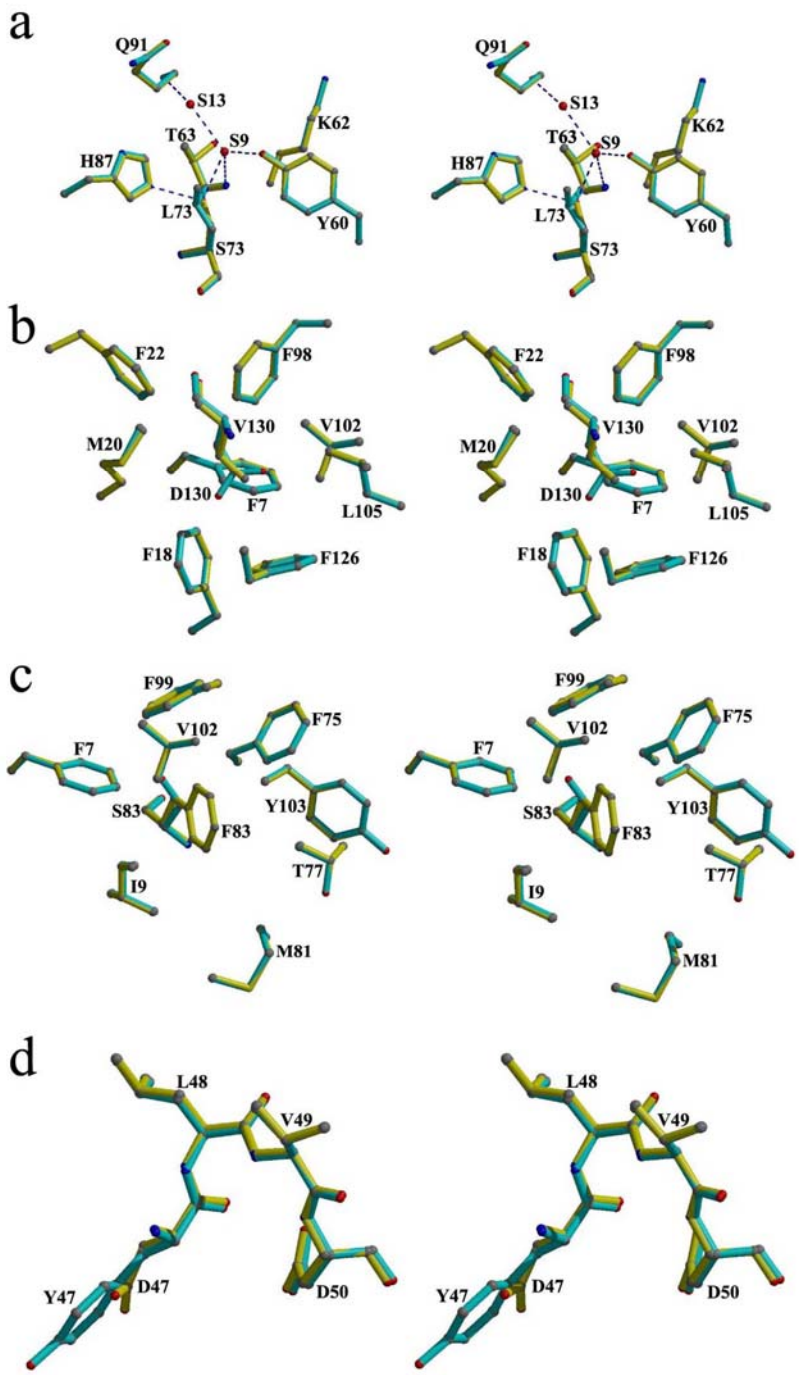

Figure 5: The detailed site stereoviews of SEDL mutations. The structures of four molecular models were superposed with wild-type. a) The region of S73L b,c) The hydrophobic environment of V130D and F83S d) The region of D47Y. The amino acids are color-coded with C in gray, O in red, N in blue, wild-type (control) in yellow, and mutations in cyan.

To visualize the structural perturbation, we built models of the SEDL mutants (S73L, V130D, F83S, and D47Y), minimized the total energy of the models, and compared them with the wild-type structure (Fig. 5). The S73, V130, and F83 residues are located at structurally important sites and buried in the helix-to-helix and helix-to-strand (Fig. 1; Jang et al. 2002a). In contrast, D47 is exposed on the surface, which area is the major area of protein-protein interaction, and which might be crucial to the conserved SEDL function. The hydroxyl group of S73 is involved in the hydrogen-bonding network, including the side chains of Y60 and H87, the backbone nitrogen atom of T63, and water molecules. Replacing a serine with hydrophobic leucine changes important properties of molecules and produces a serial disease, because this residue position cannot be incorporated without disrupting the structure of SEDL. V130 and F83 are found in completely hydrophobic environments in the interior of the protein. The structural changes of V130D and F83S mutations probably may cause functional changes in the protein. The geometries and overall stereochemical quality for four mutation structures were generated in order to compare that of wild-type. The final models exhibited r.m.s. deviations from the ideal bond angles, 1.206, 1.251, 1.221, and 1.211 for S73L, V130D, F83S, and D47Y, respectively. The r.m.s. deviation from the ideal bond lengths was the same value, 0.008 for each of the four mutations. The structural representations are shown in Figure 5. Those structures have 85.7, 85.7, 84.1, and 84.9% of amino acid residues for S73L, V130D, F83S, and D47Y in most favoured regions of a Ramachandran plot. The models of four mutations showed different geometries with r.m.s. deviations from wild-type. Also, analysis of the Ramachandran plots indicated that the mutation models present the overall stereochemical quality out of the residues from ideality in the most favored regions to compare that of wild-type.

In the case of the mutant S73L on the β4, a few residues around the mutation site, Y60, K62, T63, H87, E91 were perturbed, as shown in Figure 5a and Table 2. Whereas the interactions between β3 and α4 is mediated by water molecules in wild-type SEDL, the S73L mutation can break the interactions between β3 and α4 by disrupting hydrogen bonding; it induces a significant structural disruption and the exposure of hydrophobic amino acids and causes aggregation. In the V130D mutant, a structural perturbation was observed in the β1 (F7), β2 (F18, M20), β4 (F22, F98), α2 (F98, V102, L105), and α3 (F126) (Fig. 5b and Table 2). The large structural perturbations were mainly in helices α2 and α3. Also, we can guess that the F83S mutation induced a

significant conformational change in SEDL and that the structural perturbations were localized in the β1 (F7 and I9), β4 (F75), α1 (T77), α2 (F99, V102, and Y103), and the loop (M81) (Fig. 5c). By contrast, the D47Y mutation between α1 and β3 showed a large structural perturbation by the substitution of no charge and bulky amino acids. This indicates that a single amino acid substitution can break normal signal transduction by disrupting electrostatic interaction.

Table 2: Selected amino acids in hydrogen bonding interactions of four mutants

Mutants	S73L (β4)	V130D (α3)	F83S (β5)	D47Y (loop)
	S2	F7 (β1)	F7 (β1)	I48 (loop)---α1
	S21	F18 (β2)	I9 (β1)	V49 (loop)
	Y60 (β3)	M20 (β2)	F75 (β4)	D50 (loop)---β3
	K62 (β3)	F22 (β4)	T77 (α1)	
	T63 (β3)	F98 (α2)	M81 (loop)	
	H87 (β5)	V102 (α2)	F99 (α2)	
	E91 (α4)-S13	L105 (α2)	V102 (α2)	
		F126 (α3)	Y103 (α2)	

The structural elements in parentheses indicate the sites of the amino acids. A residue name of S indicates a solvent (water) molecule.

In summary, the expression levels were observed to determine the extent to which the secondary structure can be affected by the replacements of three each amino acids in the wild-type SEDL. The expressions of the S73L and V130D mutations showed a marked decrease by aggregation in the SDS-PAGE analysis. The mutants S73L and V130D could not obtain soluble proteins, so these proteins were refolded from the inclusion body. However, the D47Y obtain as a soluble protein less than wild-type. Gécz et al. have observed that D47Y was unable to complement, whereas V130D and S73L mutations were able to complement the TRS20 deletion (Gécz et al. 2003). These complementation results fit well with the different levels of our expressions in *E. coli*. The secondary structures and conformations of the three mutants (S73L, V130D, and D47Y) were significantly

different from those of wild-type SEDL, by CD spectroscopy. To study the multifunctional role of SEDL mutations in membrane trafficking, we will further explore the structural studies of these mutant proteins and their interactions. Characterization of the SEDL and determination of the SEDL mutation structures enable functional studies of SEDL and elucidation of the pathogenesis of SEDT.

In conclusion, we have shown that the aggregation of S73L could be attributed to breakage of hydrogen bonding geometry and exposure to hydrophobic amino acids. These results indicate that the hydrogen-bond network is important for stability and normal function of the protein. The hydrogen bonding of S73 links the two polar amino acids, Y60 and Q91 to S9 and S13 water molecules. The elimination of the hydroxyl group by the replacement of S73 with leucine results in a loss of conformational stability. The S73L mutation decreased the stability and soluble expression of SEDL significantly, and exhibited a synergistic effect on the aggregation of protein relative to the respective single mutations. Additionally, we suggest that S73 cannot function efficiently alone without additional support from the hydrogen bonds of Y60 and Q91. Our results demonstrate that the hydrogen-bond network provides the structural support that is necessary for the protein to maintain the active-site geometry optimized for function and stability. The structural characterization of a SEDL protein variant with Val130 substituted for Asp suggests that the variant is trapped in a conformation that resembles the F83S mutation by modeling analysis. From these results, we confirmed that there are no bound hydrophobic amino acids and that hydrophobic interaction was lost in the V130D and F83S mutant structures. Interestingly, although the spectral shape of the D47Y mutant was similar to that of the wild-type SEDL, the slope of the plot of D47Y was significantly decreased relative to that of the wild-type, implying that the environment near D47Y might cause conformational change by the substitution of the bulky amino acid and the decrease of interaction by the loss an amino acid charge. Gécz et al. identified that there is no obvious correlation between the nature and position of the SEDL mutation and the clinical severity of the disorder among the human SEDL patients (Gécz et al. 2003). In our experiments, we have observed that four different mutations show different levels of expressions and characterization compared to that of wild-type. This may reflect the subtle impact of the mutations on SEDL protein function as previously observed among SEDL patients. Our results suggest a difference in activity and/or stability of the mutant compared to the wild-type SEDL protein.

Acknowledgements

This work was supported by Korea Research Foundation Grant (KRF-2002-041-C00244).

References

Bannerman, R.M., Ingall, G.B. and Mohn, J.F. (1971) J. Med Genet. 8, 291-301.

Iceton, J.A. and Horne, G. J. (1986) Bone Joint Surg. [Br] 68 616-619.

MacKenzie, J.J., Fitzpatrick, J., Babyn, P., Ferrero, G.B., Ballabio, A., Billingsley, G., Bulman, D.E., Strasberg, P., Ray, P.N., and Costa, T. (1996) J. Med. Genet. 33, 823-828.

Gedeon, A.K., Colley, A., Jamieson, R., Thompson, E.M., Rogers, J., Sillence, D., Tiller, G.E., Mulley, J.C., and Gécz, (1999) J. Nat. Genet. 22, 400-404.

Sacher, M. and Ferro-Novick, S. (2001) Methods Enzymol. 329, 234-241.

Sacher, M. (2003) FEBS Letters 550, 1-4.

Shi, Y.-R., Lee, C.-C., Hsu, Y.-A., Wang, C.-H. and Tsai, F.-J. (2002) Hum. Hered. 54, 54-56.

Fiedler, J., Bittner, M., Puhl, W. and Brenner, R.E. (2002) Clin. Genet. 62, 94-95.

Shaw, M.A., Brunetti-Pierri, N., Kadasi, L., Kovacova, V., an Maldergem Van V L., De Brasi, D. and Salerno, M., Gecz, J. (2003) Clin. Genet. 64, 235-242.

Xiao, C., Zhang, S., Wang, J., Qiu, W., Chi, L., Li, Y. and Su, Z. (2003) Mutation Research 525, 61-65.

Shaw, M.A., McDonough, B., Hodess, A.B., Harter, D.H. and Gecz, J. (2004) Am. J. Med. Genet. 129A, 206-207.

Fiedler, J., Le Merrer, M., Mortier, G., Heuertz, S., Faivre, L. and Brenner (2004) R.E. Hum. Mutat. 24, 103.

Bar-Yosef, U., Ohana, E., Hershkovitz, E., Perlmuter, S., Ofir, R. and Birk, O.S. (2004) Am. J. Med. Genet. 125A, 45-48.

Jang, S.B., Kim, Y.-G., Cho, Y.-S., Suh, P.-G., Kim, K.-H. and Oh, B.-H. (2002a) J. Biol. Chem. 277, 49863-49869.

Jang, S.B., Cho, Y.-S., Eom, S.-J., Choi, E.-J., Kim, K.-H., Suh, P.-G. and Oh, B.-H. (2002b) Acta Crystallogr. D58, 564-566.

Gharahdaghi, F., Weinberg, C. R., Meagher, D. A., Imai, B. S. and Mische, S. M. (1999) Electrophoresis 20**,** 601–605.

Jones, T.A., Zou, J.Y., Cowan, S.W. and Kjeldgaard, M. (1991) Acta Crystallogr. A47, 110-119.

Brunger, A.T., Adams, P. D., Clore, G.M., DeLano, W.L., Gros, P., Grosse-Kunstleve, R.W., Jiang, J.S., Kuszewski, J., Nilges, M.,

Pannu, N.S., Read, R.J., Rice, L.M., Simonson, T. and Warren, G.L. (1998) Acta Crystallogr. D54, 905-921.

Laskowski, R.A., McArthur, M.W., Moss, D.S., and Thornton, J.M. (1993) J. Appl. Crystallogr. 24, 946-950.

Grunebaum, E., Arpaia, E., MacKenzie, J. J., Fitzpatrick, J., Ray, P.N., Roifman, C.M. (2001) J. Med. Genet. 38, 409-411.

Garnier, J., Gibrat, J.F., Robson, B. (1999) GOR secondary structure prediction method version IV. Methods in enzymology vol 266. San Diego: Doolittle, 540-553.

Guermeur, Y. Combinaison de classifieurs statistiques, application a la prediction de structure secodarie des proteins. PhD thesis. Pole Bio-informatique Lyonnais Network protein Sequence Analysis.

Frishman, D., Argus, P. (1996) Protein Eng. 9, 133-142.

Whyte, M.P., Gottesman G.S., Eddy, M.C., McAlister, W.H. (1999) Medicine, 78, 9-25.

Bannerman, R.M., Ingall, G.B., Mohn, J.F. (1971) J. Med. Genet. 8, 291-310.

Gécz, J., Shaw, M.A., Bellon, J.R., Lopes, M.de.B. (2003) Gene 320, 137-144.